Elucidating the local structure of $Li_{1+x}Al_xTi_{2-x}(PO_4)_3$ and $Li_3Al_xTi_{2-x}(PO_4)_3$ (x = 0, 0.3) *via* total scattering

Matthew S. Chambers*[a], Jue Liu[b], Olaf J, Borkiewicz[c], Kevin Llopart[a], Robert L Sacci[a] ,Gabriel M. Veith*[a]

[a]Chemical Sciences division, Oak Ridge National Laboratory, Oak Ridge, Tennessee 37831, United States

[b] Neutron Scattering Division, Oak Ridge National Laboratory, Oak Ridge, Tennessee 37831, United States

[c] X-ray Science Division, Advanced Photon Source, Argonne National Laboratory, Lemont, Illinois 60439, United States

Corresponding authors' e-mail addresses:

chambersms1@ornl.gov (Matthew S. Chambers), veithgm@ornl.gov (Gabriel M. Veith)

Supporting Information

$Li_3Ti_2(PO_4)_3$ appearance

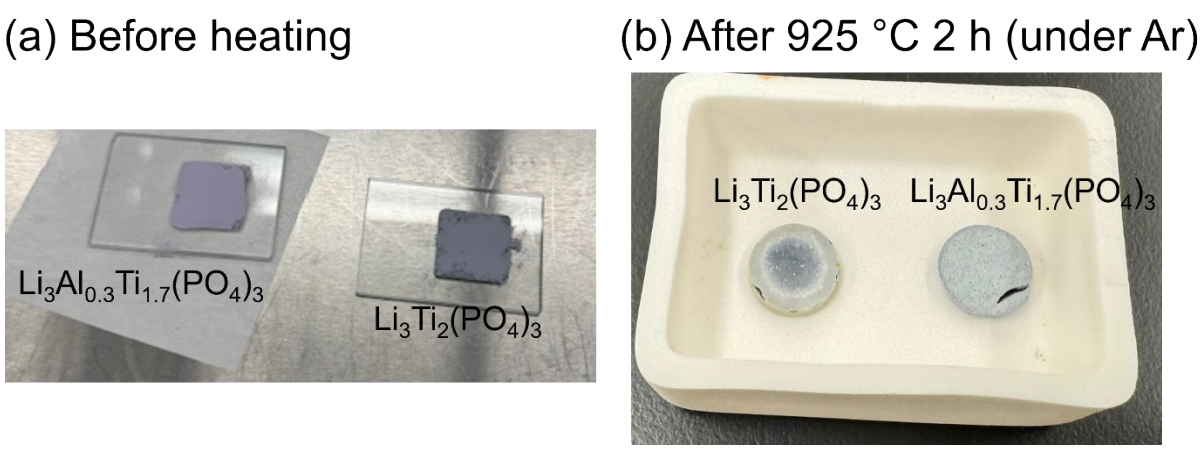

Figure S1 – Appearance of $Li_3Al_xTi_{2-x}(PO_4)_3$ (x =0, 0.3) (a) Before heating; (b) after heating at 925 °C under Ar for 2 h with heating and cooling rates of 5 °C min^{-1}.

X-ray total scattering sample holders and heating environment

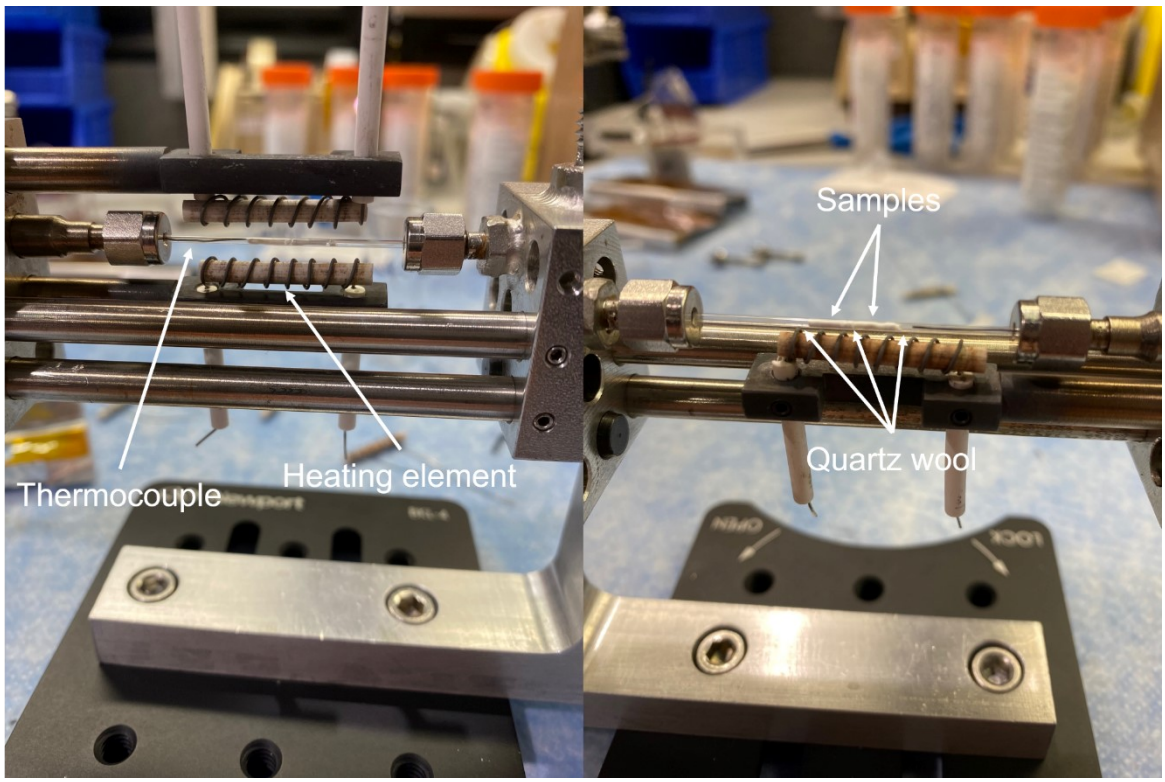

Figure S2 – Sample holders used in the X-ray total scattering experiment.

Laboratory X-ray patterns

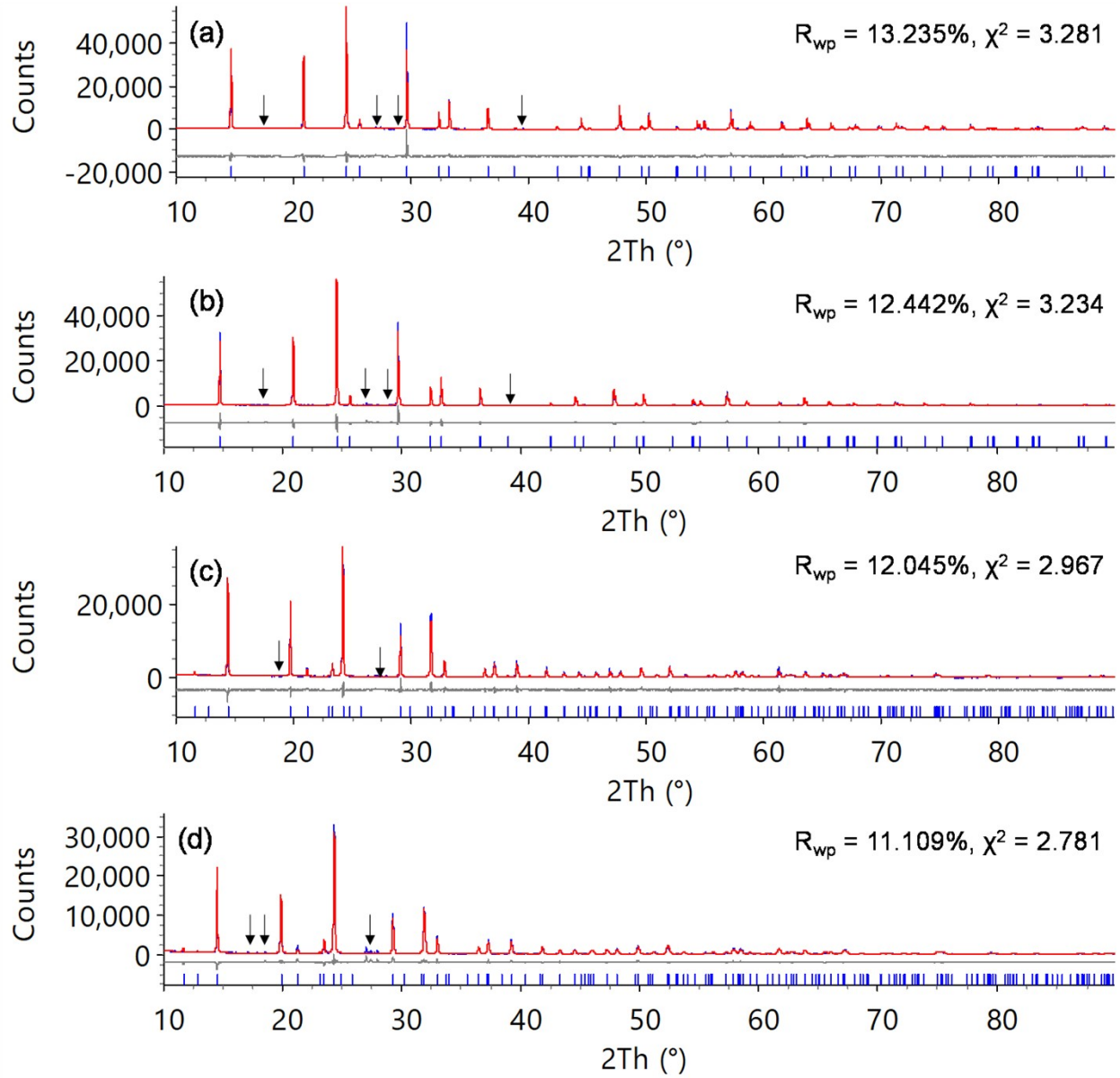

Figure S3 – Rietveld plots of $Li_{1+x}Al_xTi_{2-x}(PO_4)_3$ and $Li_3Al_xTi_{2-x}(PO_4)_3$ synthesized through the solid-state method. (a) $LiTi_2(PO_4)_3$; (b) $Li_{1.3}Al_{0.3}Ti_{1.7}(PO_4)_3$; (c) $Li_3Ti_2(PO_4)_3$; (d) $Li_3Al_{0.3}Ti_{1.7}(PO_4)_3$. Blue curves = observed data; red curves = calculated pattern; grey curves = difference between observed and calculated. Blue tick marks correspond to reflections arising from $Li_{1+x}Al_xTi_{2-x}(PO_4)_3$ or $Li_3Al_xTi_{2-x}(PO_4)_3$. Black arrows indicate unaccounted peaks.

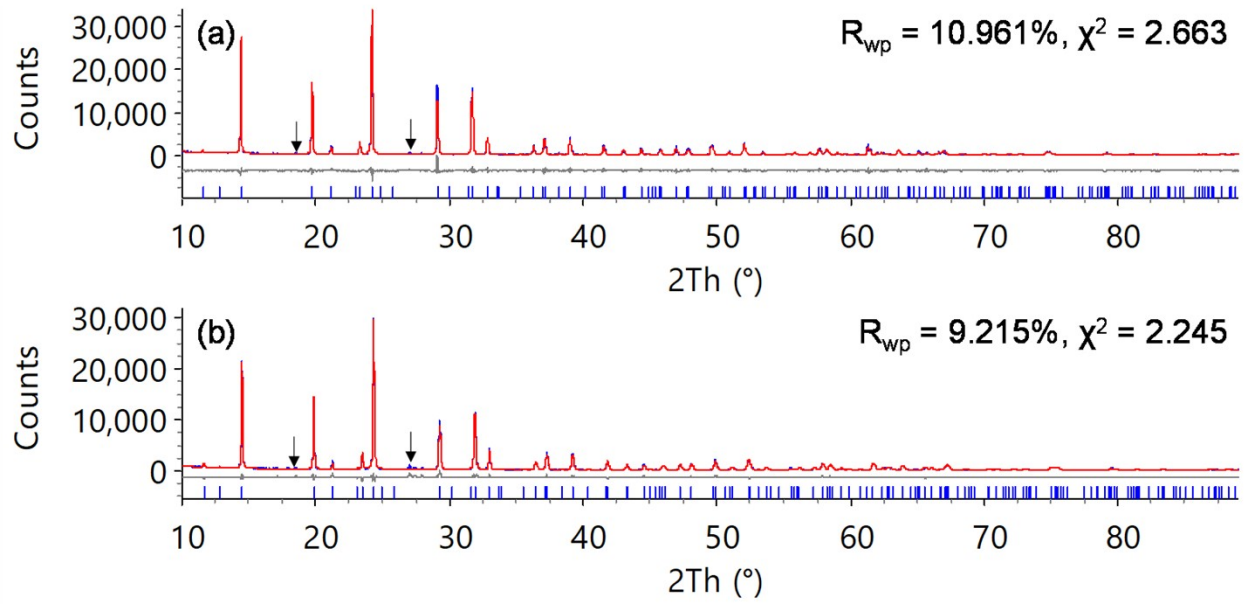

Figure S4 – Laboratory X-ray Rietveld plots of $Li_3Al_xTi_{2-x}(PO_4)_3$ (x = 0, 0.3) made for conductivity measurements; (a) $Li_3Ti_2(PO_4)_3$; (b) $Li_3Al_{0.3}Ti_{1.7}(PO_4)_3$. Blue curves = observed data; red curves = calculated pattern; grey curves = difference between observed and calculated. Blue tick marks correspond to reflections arising from $Li_3Al_xTi_{2-x}(PO_4)_3$. Black arrows indicate unaccounted peaks.

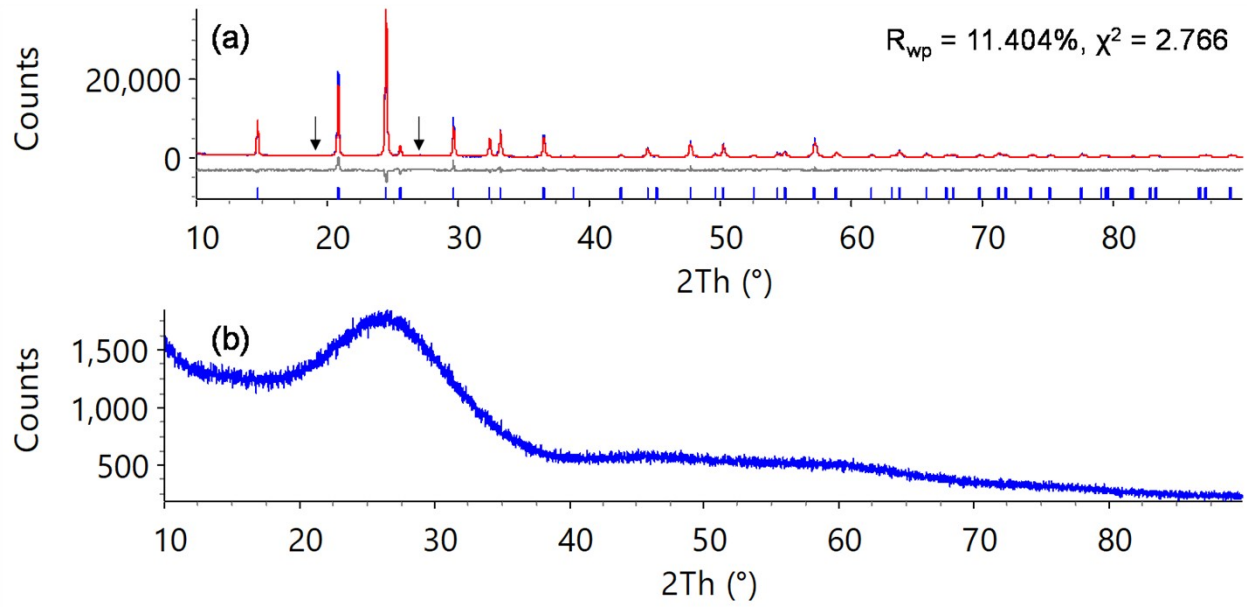

Figure S5 – Laboratory X-ray Rietveld plot and diffraction patterns of sol-gel-synthesized $LiTi_2(PO_4)_3$. (a) $LiTi_2(PO_4)_3$ heated to 800 °C; (b) $LiTi_2(PO_4)_3$ heated to 300 °C.

Sol-gel synchrotron Bragg scattering patterns

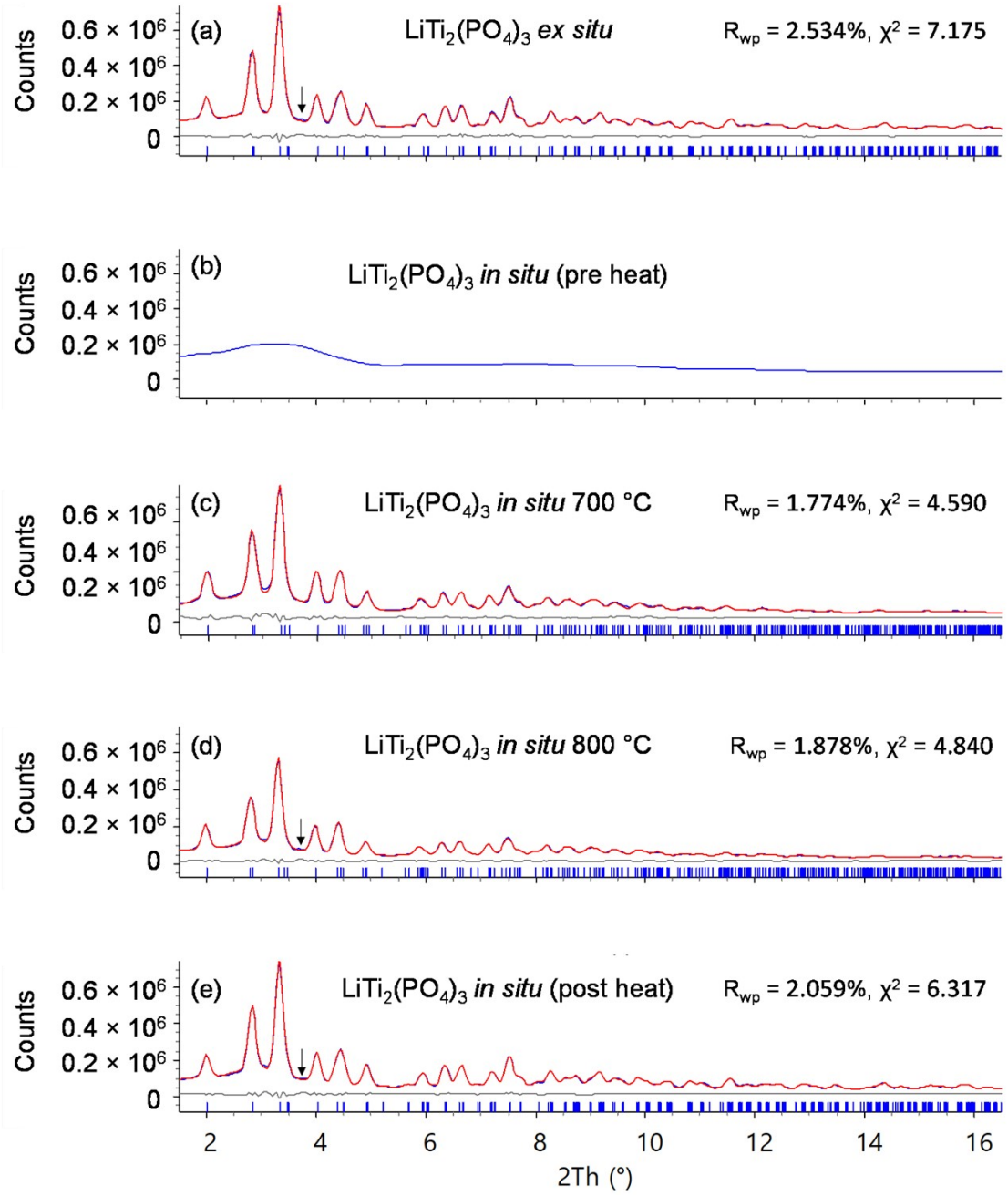

Figure S6 – Synchrotron Rietveld plots and powder patterns for sol-gel syntheses of $LiTi_2(PO_4)_3$ at 25 °C (a) *ex situ* sol-gel $LiTi_2(PO_4)_3$; (b) *in situ* $LiTi_2(PO_4)_3$ pre-heating; (c) *in situ* $LiTi_2(PO_4)_3$ at 700 °C; (d) *in situ* $LiTi_2(PO_4)_3$ at 800 °C; (e) *in situ* $LiTi_2(PO_4)_3$ post-heating. Blue curves = observed data; red curves = calculated patterns; grey curves = difference between observed and calculated patterns; blue tick marks = reflections arising from $LiTi_2(PO_4)_3$. For (b), the pattern largely derives from the quartz capillary.

***In-situ* sol-gel XPDF**

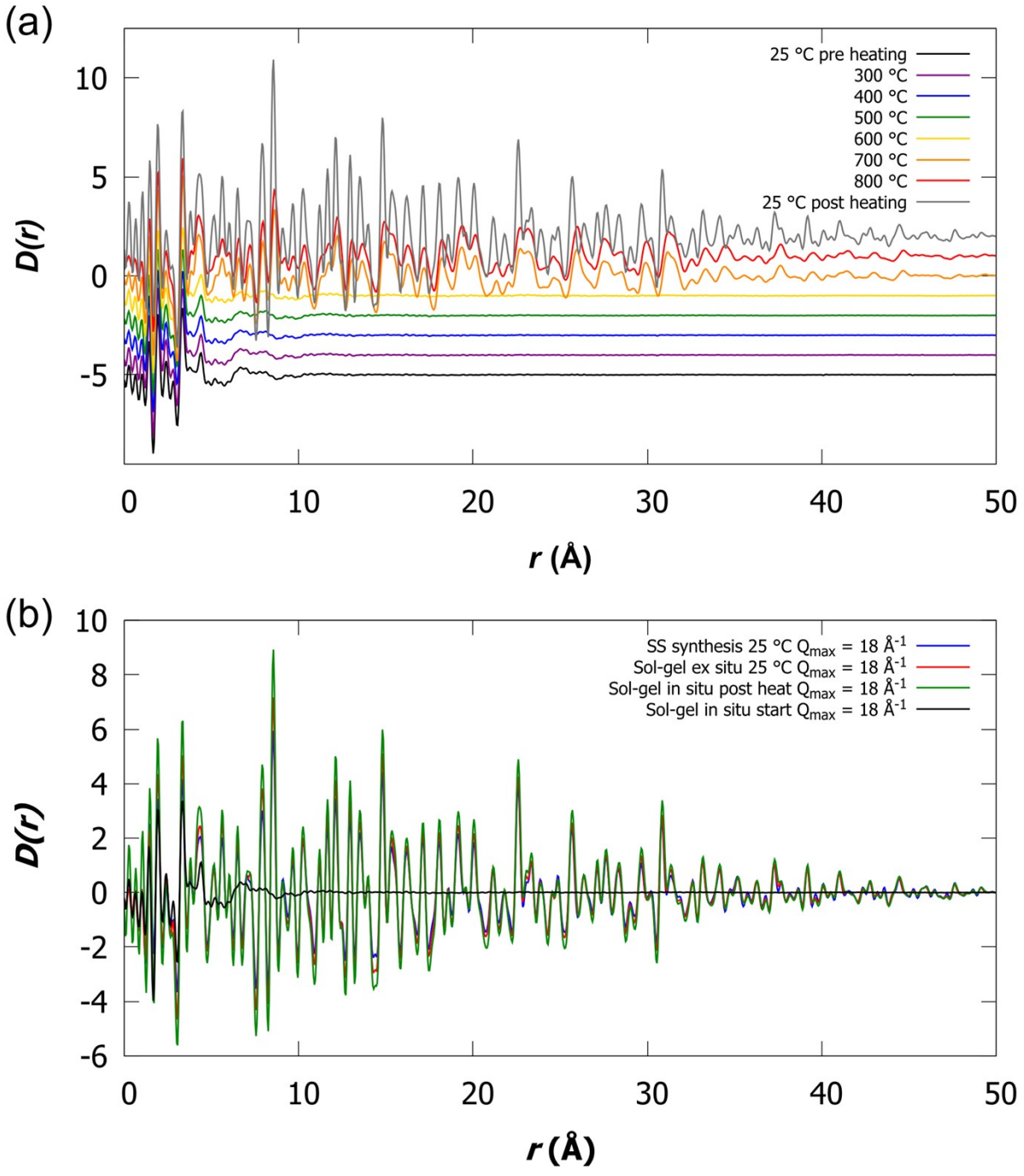

Figure S7 – X-ray PDF patterns of $LiTi_2(PO_4)_3$ as synthesized using the sol-gel and solid-state method; (a) *in situ* sol-gel X-PDF across the whole *r* range; (b) *ex situ* sol-gel, *in situ* sol-gel and *in situ* sol-gel post-heating.

Neutron Rietveld refinements

Table S1 – selected bond distances for $LiTi_2(PO_4)_3$ given in Å

	O1	**O2**
Ti1	1.8823(11)	1.9812(11)
P1	1.5349(8)	1.5218(6)
Li1	N/A	2.2707(5)

Table S2 – selected bond distances for $Li_{1.32(5)}Al_{0.3}Ti_{1.7}(PO_4)_3$

	O1	**O2**
Ti1/Al1	1.8801(18)	1.977(2)
P1	1.5349(8)	1.5246(9)
Li1	N/A	2.2760(7)
Li2	2.20(5)	2.12(9)

Table S3 – selected bond distances for $Li_{3.01(4)}Ti_2(PO_4)_3$

	O1	**O2**	**O3**	**O4**
Ti1	2.056(3)	N/A	2.026(3)	N/A
Ti2	N/A	2.056(3)	N/A	2.048(3)
P1	1.5392(16)	1.5214(19)	1.532(2)	1.545(2)
Li1	2.026(6)	2.000(5)	N/A	1.979(5)
Li2	2.002(17)	1.939(19)	2.17(2)	3.13(3)

Table S4 – selected bond distances for $Li_{2.96(5)}Al_{0.273(7)}Ti_{1.727(7)}(PO_4)_3$

	O1	**O2**	**O3**	**O4**
Ti1/Al1	2.005(4)	N/A	2.012(4)	N/A
Ti2/Al2	N/A	2.061(4)	N/A	2.017(4)
P1	1.5385(18)	1.511(2)	1.543(2)	1.551(3)
Li1	1.981(6)	1.994(5)	N/A	1.979(7)
Li2	2.13(3)	2.04(3)	2.06(3)	2.77(3)

Neutron PDFs

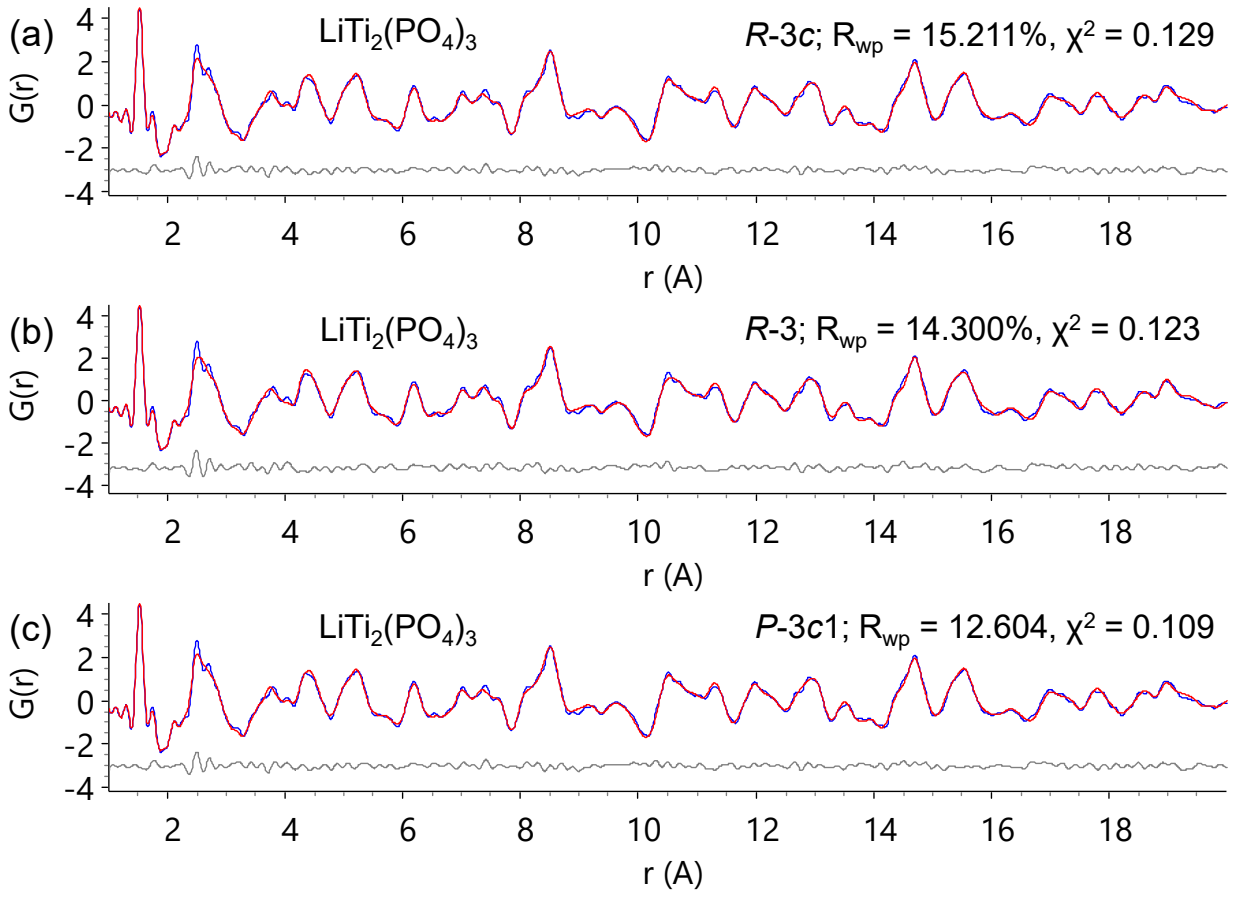

Figure S8 – Small box neutron PDF refinements of $LiTi_2(PO_4)_3$ using (a) *R*-3*c* symmetry, (b) *R*-3 symmetry and (c) *P*-3*c*1 symmetry. Blue curves = observed PDF, red curves = calculated PDF, grey curves = difference between observed and calculated PDFs.

Table S5 – structural parameters for $LiTi_2(PO_4)_3$ obtained from small box PDF refinements. Space group = *P*-3*c*1; a = 8.5034(9) Å, c = 20.821(4) Å, α = 90°, γ = 120°, V = 1303.9(4) Å^3, R_{wp} = 12.604%, χ^2 = 0.109

Site label	**Wyckoff site**	***x***	***y***	***z***	**Occupancy**
Ti1_1	4*c*	0	0	0.1381(7)	1
Ti1_2	4*d*	1/3	2/3	0.4760(4)	1
Ti1_3	4*d*	1/3	2/3	0.6923(5)	1
P1_1	6*f*	0.7135(7)	0	¼	1
P1_2	12*g*	0.3351(5)	0.3756(5)	0.5855(2)	1
O1_1	12*g*	–0.0006(9)	0.8064(5)	0.1878(2)	1
O1_2	12*g*	0.3316(7)	0.4811(6)	0.5261(2)	1
O1_3	12*g*	0.6511(10)	0.1402(10)	0.8554(3)	1
O2_1	12*g*	0.1589(7)	–0.0349(8)	0.0842(3)	1
O2_2	12*g*	0.5034(4)	0.6480(5)	0.4141(3)	1
O2_3	12*g*	0.8287(6)	0.3153(9)	0.7456(2)	1
Li1_1	2*b*	0	0	0	1
Li1_2	4*d*	1/3	2/3	0.336(13)	1

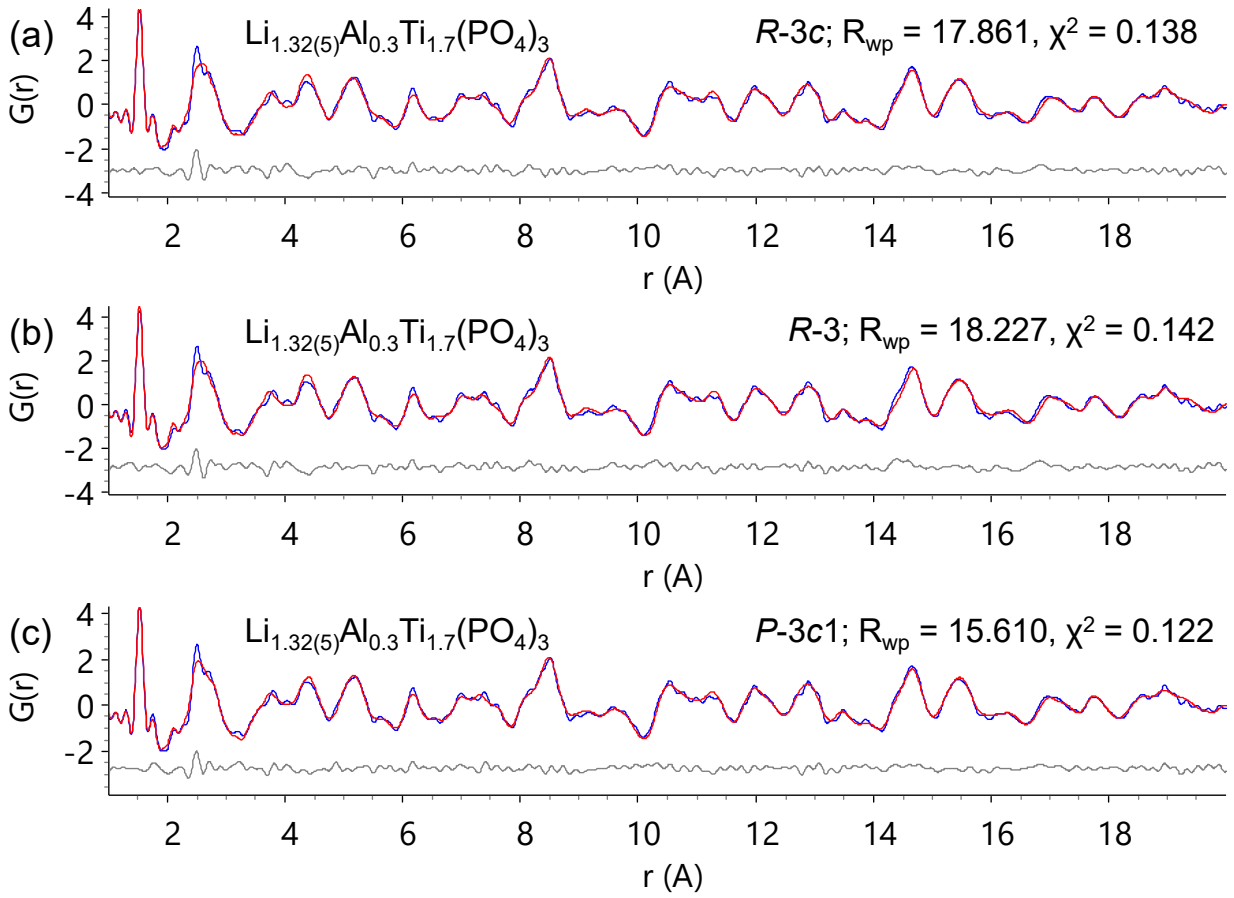

Figure S9 – Small box neutron PDF refinements of $Li_{1.32(5)}Al_{0.3}Ti_{1.7}(PO_4)_3$ using (a) *R*-3*c* symmetry, (b) *R*-3 symmetry and (c) *P*-3*c*1 symmetry. Blue curves = observed PDF, red curves = calculated PDF, grey curves = difference between observed and calculated PDFs.

Table S6 – structural parameters for $Li_{1.32(5)}Al_{0.3}Ti_{1.7}(PO_4)_3$ obtained from small box PDF refinements. Space group = *P*-3*c*1; a = 8.4895(15) Å, c = 20.780(6) Å, α = 90°, γ = 120°, V = 1297.0(6) Å^3, R_{wp} = 15.610%, χ^2 = 0.122

Site label	**Wyckoff site**	***x***	***y***	***z***	**Occupancy**
Ti1_1	4*c*	0	0	0.1356(13)	0.85
Al1_1	4*c*	0	0	0.1356(13)	0.15
Ti1_2	4*d*	1/3	2/3	0.4760(10)	0.85
Al1_2	4*d*	1/3	2/3	0.4760(10)	0.15
Ti1_3	4*d*	1/3	2/3	0.6943(12)	0.85
Al1_3	4*d*	1/3	2/3	0.6943(12)	0.15
P1_1	6*f*	0.7124(18)	0	¼	1
P1_2	12*g*	0.3356(13)	0.3748(8)	0.5865(3)	1
O1_1	12*g*	0.0005(18)	0.810(2)	0.1887(7)	1
O1_2	12*g*	0.3276(16)	0.4754(17)	0.5240(5)	1
O1_3	12*g*	0.6523(13)	0.1384(13)	0.8557(3)	1
O2_1	12*g*	0.1630(17)	–0.027(2)	0.0846(6)	1
O2_2	12*g*	0.4971(19)	0.645(2)	0.4146(7)	1
O2_3	12*g*	0.8305(13)	0.3145(16)	0.7450(5)	1
Li1_1	2*b*	0	0	0	0.85
Li1_2	4*d*	1/3	2/3	0.335(19)	0.85
Li2_1	12*g*	0.28(2)	0.187(18)	0.047(7)	0.077
Li2_2	12*g*	0.636(13)	–0.058(12)	0.384(5)	0.077
Li2_3	12*g*	0.092(11)	0.699(12)	0.780(5)	0.077

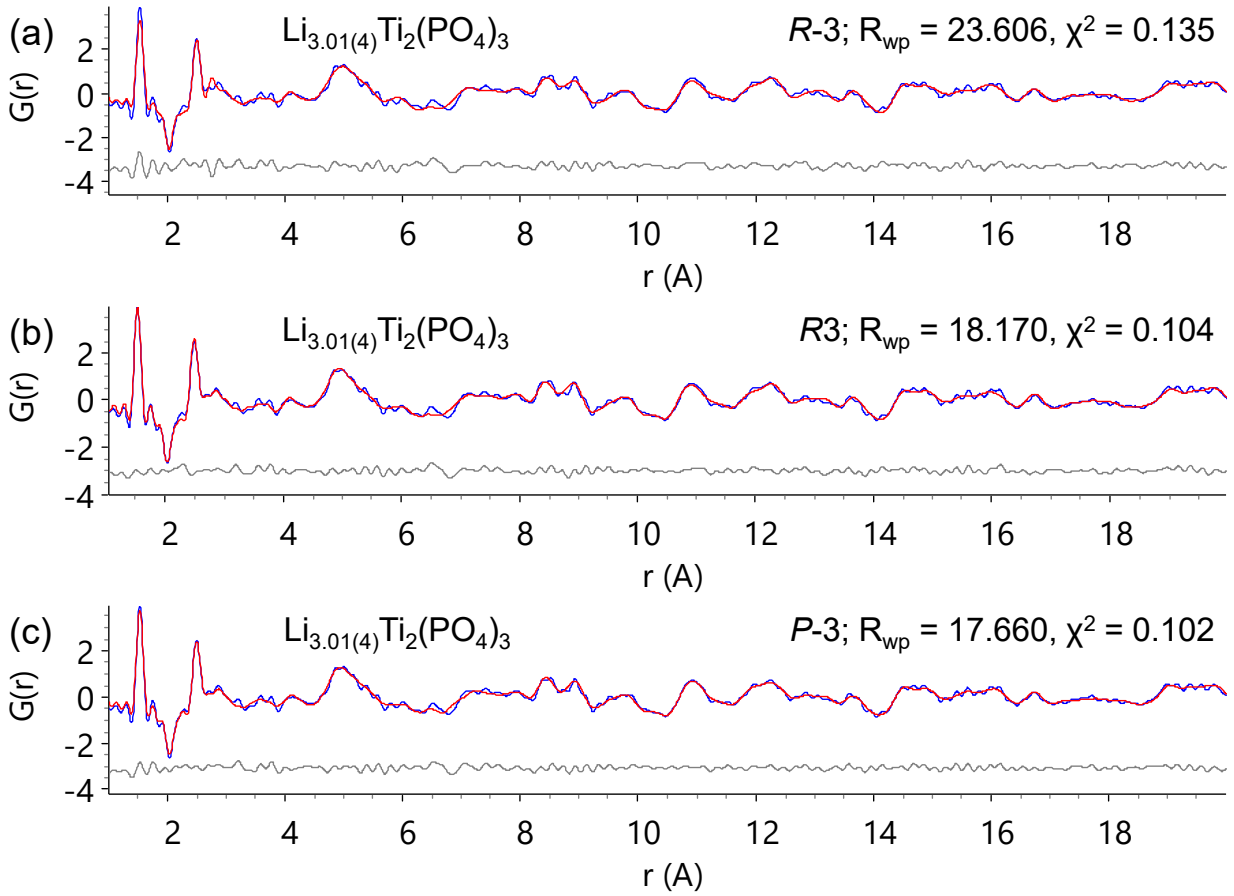

Figure S10 – Small box neutron PDF refinements of $Li_{3.01(4)}Ti_2(PO_4)_3$ using (a) *R*-3 symmetry, (b) *R*3 symmetry and (c) *P*-3 symmetry. Blue curves = observed PDF, red curves = calculated PDF, grey curves = difference between observed and calculated PDFs.

Table S7 – structural parameters for $Li_{3.01(4)}Ti_2(PO_4)_3$ obtained from small box PDF refinements. Space group = *P*-3; a = 8.376(2) Å, c = 22.808(10) Å, α = 90°, γ = 120°, V = 1385.9(9) Å^3, R_{wp} = 17.666%, χ^2 = 0.102

Site label	**Wyckoff site**	***x***	***y***	***z***	**Occupancy**
Ti1_1	2*c*	0	0	0.145(4)	1
Ti1_2	2*d*	1/3	2/3	0.479(5)	1
Ti1_3	2*d*	1/3	2/3	0.215(2)	1
Ti2_1	2*c*	0	0	0.352(3)	1
Ti2_2	2*d*	1/3	2/3	0.684(4)	1
Ti2_3	2*d*	1/3	2/3	–0.015(3)	1
P1_1	6*g*	0.002(5)	0.716(3)	0.2500(17)	1
P1_2	6*g*	0.330(5)	0.371(4)	0.5848(12)	1
P1_3	6*g*	0.667(4)	0.040(5)	–0.0845(15)	1
O1_1	6*g*	0.213(5)	0.052(4)	0.0918(11)	1
O1_2	6*g*	0.547(5)	0.716(5)	0.4233(15)	1
O1_3	6*g*	0.887(4)	0.385(5)	0.7538(11)	1
O2_1	6*g*	0.895(3)	0.411(3)	0.0598(10)	1
O2_2	6*g*	0.237(3)	0.112(3)	0.4055(9)	1
O2_3	6*g*	0.563(4)	0.757(3)	0.7321(12)	1
O3_1	6*g*	–0.002(4)	0.801(5)	0.1931(12)	1
O3_2	6*g*	0.329(4)	0.468(4)	0.5280(12)	1
O3_3	6*g*	0.658(4)	0.138(4)	0.8616(13)	1
O4_1	6*g*	0.137(3)	0.227(3)	0.2979(12)	1
O4_2	6*g*	0.481(4)	–0.103(3)	0.6316(10)	1
O4_3	6*g*	0.820(3)	0.580(2)	–0.0333(12)	1
Li1_1	6*g*	0.316(16)	0.290(16)	0.044(4)	0.8902
Li1_2	6*g*	0.638(10)	–0.051(9)	0.387(3)	0.8902
Li1_3	6*g*	–0.023(15)	0.625(16)	0.708(3)	0.8902
Li2_1	6*g*	0.71(4)	0.14(4)	0.114(13)	0.19527
Li2_2	6*g*	0.06(4)	0.81(4)	0.470(11)	0.19527
Li2_3	6*g*	0.40(4)	0.46(5)	0.812(13)	0.19527

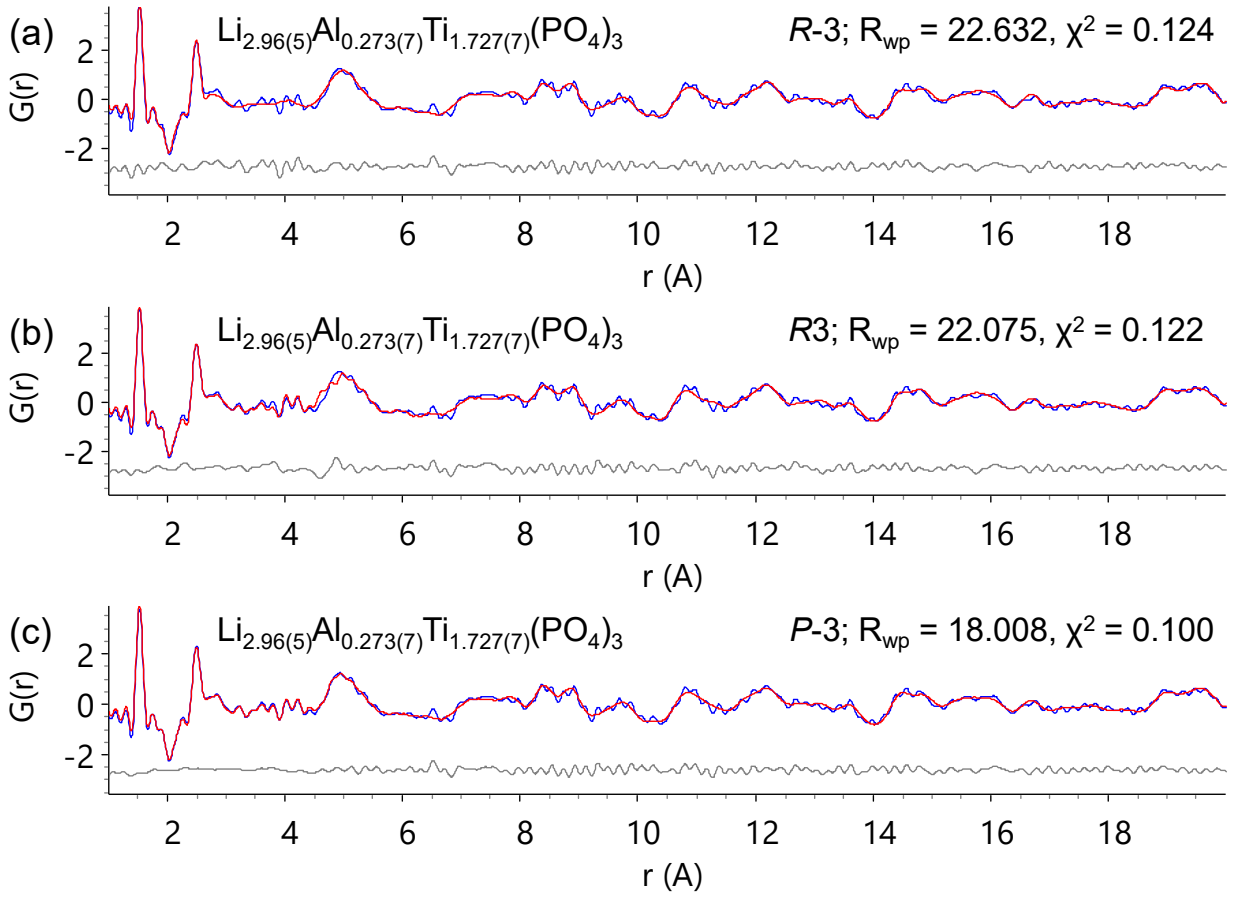

Figure S11 – Small box neutron PDF refinements of $Li_{2.96(5)}Al_{0.273(7)}Ti_{1.727(7)}(PO_4)_3$ using (a) *R*-3 symmetry, (b) *R3* symmetry and and (b) *P*-3 symmetry. Blue curves = observed PDF, red curves = calculated PDF, grey curves = difference between observed and calculated PDFs.

Table S8 – structural parameters for $Li_{2.96(5)}Al_{0.273(7)}Ti_{1.727(7)}(PO_4)_3$ obtained from small box PDF refinements. Space group = *P*-3; a = 8.347(2) Å, c = 22.591(13) Å, α = 90°, γ = 120°, V = 1363.3(11) Å^3, R_{wp} = 17.666%, χ^2 = 0.102

Site label	Wyckoff site	*x*	*y*	*z*	Occupancy
Ti1_1	2*c*	0	0	0.141(3)	0.87041
Al1_1	2*c*	0	0	0.141(3)	0.12959
Ti1_2	2*d*	1/3	2/3	0.471(3)	0.87041
Al1_2	2*d*	1/3	2/3	0.471(3)	0.12959
Ti1_3	2*d*	1/3	2/3	0.191(3)	0.87041
Al1_3	2d	1/3	2/3	0.191(3)	0.12959
Ti2_1	2*c*	0	0	0.352(5)	0.85617
Al2_1	2*c*	0	0	0.352(5)	0.14383
Ti2_2	2*d*	1/3	2/3	0.686(5)	0.85617
Al2_2	2*d*	1/3	2/3	0.686(5)	0.14383
Ti2_3	2*d*	1/3	2/3	–0.019(3)	0.85617
Al2_3	2*d*	1/3	2/3	–0.019(3)	0.14383
P1_1	6*g*	–0.004(5)	0.709(4)	0.2502(10)	1
P1_2	6*g*	0.330(3)	0.369(3)	0.5888(9)	1
P1_3	6*g*	0.667(4)	0.043(3)	-0.0839(8)	1
O1_1	6*g*	0.214(3)	0.045(2)	0.0907(6)	1
O1_2	6*g*	0.549(3)	0.721(3)	0.4192(9)	1
O1_3	6*g*	0.884(3)	0.386(2)	0.7569(10)	1
O2_1	6*g*	0.9021(18)	0.4349(18)	0.0729(6)	1
O2_2	6*g*	0.226(2)	0.0943(19)	0.3985(11)	1
O2_3	6*g*	0.565(3)	0.758(2)	0.7280(9)	1
O3_1	6*g*	–0.013(2)	0.811(2)	0.1939(7)	1
O3_2	6*g*	0.340(2)	0.477(2)	0.5284(7)	1
O3_3	6*g*	0.665(3)	0.145(3)	0.8625(9)	1
O4_1	6*g*	0.149(3)	0.230(3)	0.2990(8)	1
O4_2	6*g*	0.474(3)	-0.101(3)	0.6338(6)	1
O4_3	6*g*	0.818(2)	0.5761(14)	–0.0329(8)	1
Li1_1	6*g*	0.722(8)	0.037(7)	0.049(3)	0.807
Li1_2	6*g*	0.032(6)	0.671(4)	0.371(2)	0.807
Li1_3	6*g*	0.388(6)	0.359(5)	0.721(2)	0.807
Li2_1	6*g*	0.34(3)	0.36(2)	0.132(9)	0.179
Li2_2	6*g*	0.71(3)	0.06(3)	0.467(9)	0.179
Li2_3	6*g*	0.07(3)	0.69(3)	0.804(9)	0.179

X-ray diffraction patterns of $Li_{1+x}Al_xTi_{2-x}(PO_4)_3$ and $Li_3Al_xTi_{2-x}(PO_4)_3$ (x = 0, 0.3) samples made for electrochemical impedance measurements

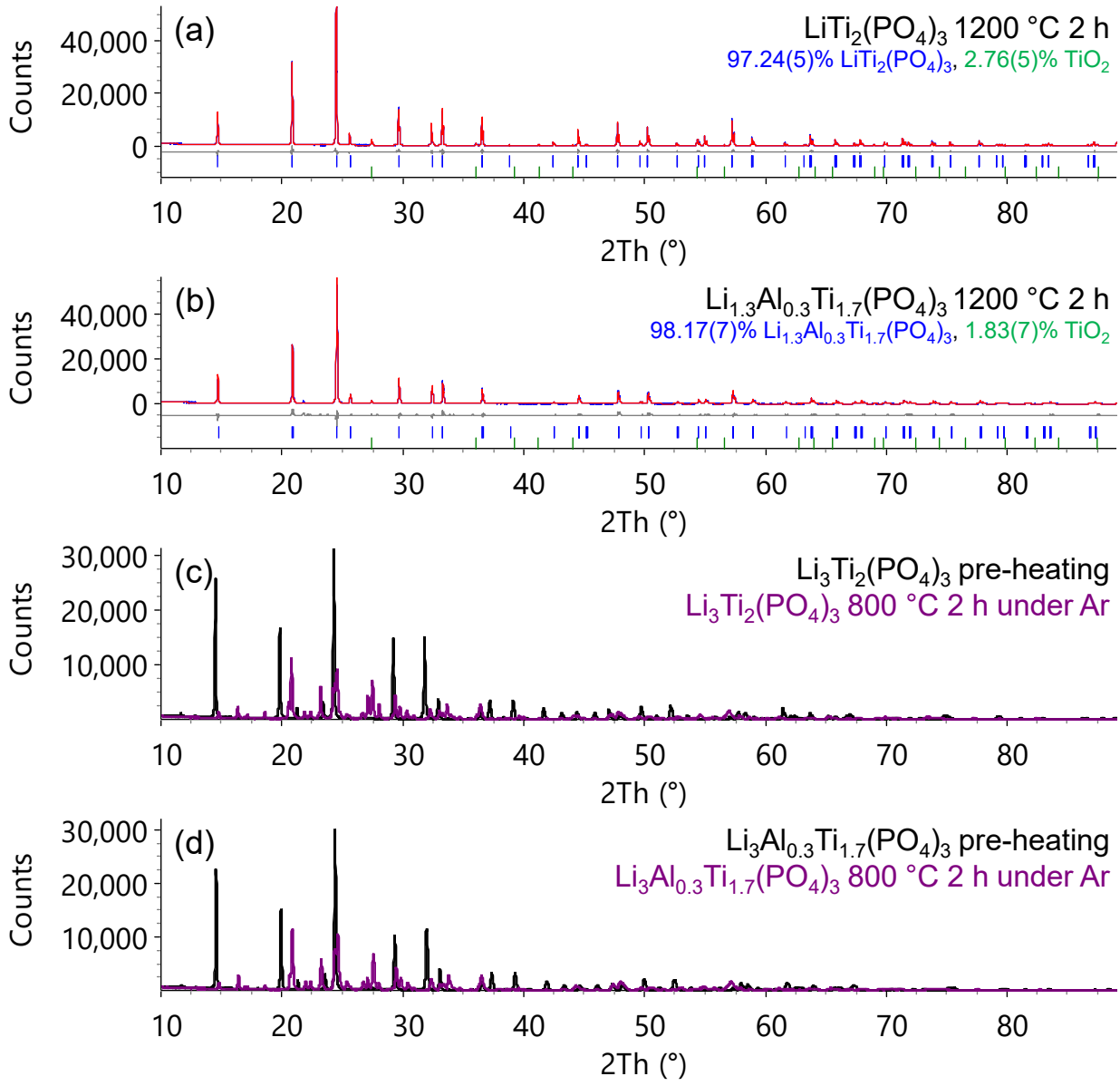

Figure S12 – (a – b) Rietveld plots of $Li_{1+x}Al_xTi_{2-x}(PO_4)_3$ and (c – d) raw X-ray diffraction patterns of $Li_3AlxTi_{2-x}(PO_4)_3$ (x = 0, 0.3) sintered pellets; (a) $LiTi_2(PO_4)_3$ heated to 1200 °C for 2 h (b) $Li_{1.3}Al_{0.3}Ti_{1.7}(PO_4)_3$ heated to 1200 °C 2 h; blue curves = observed data, red curves = calculated pattern; grey curves = difference between calculated and observed data; blue tick marks = reflections arising from NASICON structure; green tick marks = reflections from TiO_2. (c) $Li_3Ti_2(PO_4)_3$ before heating and after heating to 800 °C for 2 h; (d) $Li_3Al_{0.3}Ti_{1.7}(PO_4)_3$ before heating and after heating to 800 °C for 2 h; black curves = before heating; purple curves = after heating. Heating and cooling rates in all samples were ±5 °C min^{-1}.

Electrochemical impedance spectra

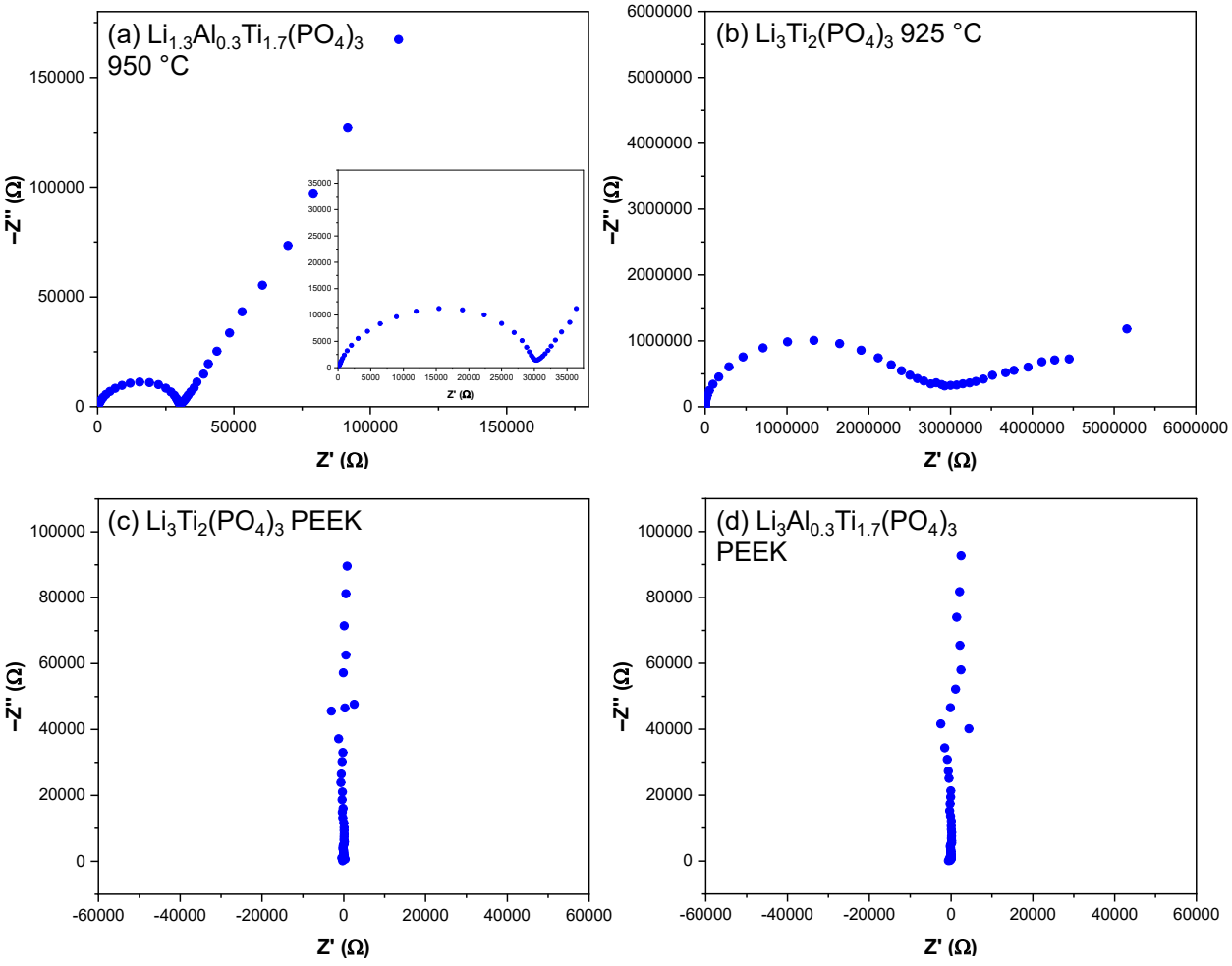

Figure S13 – Nyquist plots of (a) $Li_{1.3}Al_{0.3}Ti_{1.7}(PO_4)_3$ sintered at 950 °C for 6 h; (b) $Li_3Ti_2(PO_4)_3$ sintered at 925 °C for 2 h under flowing Ar; (c) PEEK cell measurement of $Li_3Ti_2(PO_4)_3$; (d) PEEK cell measurement of $Li_3Al_{0.3}Ti_{1.7}(PO_4)_3$. (c – d) show a similar response of pure capacitors, suggesting that there was no cold-sintering of the "pellets" in the PEEK cell.